LA-UR-17-23912
Approved for public release; distribution is unlimited.

Title: Fine Tuning the CJ Detonation Speed of a High Explosive products Equation of State

Author(s): Menikoff, Ralph

Intended for: Report

Issued: 2018-06-29 (rev.2)

Fine Tuning the CJ Detonation Speed of a High Explosive products Equation of State

Ralph Menikoff

June 22, 2018

Abstract

For high explosive (HE) simulations, inaccuracies of a per cent or two in the detonation wave speed can result from not sufficiently resolving the reaction-zone width or from small inaccuracies in calibrating the products equation of state (EOS) or from variation of HE lots. More accurate detonation speeds can be obtained by fine tuning the equation of state to compensate. Here we show that two simple EOS transformations can be used to adjust the CJ detonation speed by a couple of per cent with minimal effect on the CJ release isentrope. The two transformations are (1) a shift in the energy origin and (2) a linear scaling of the specific volume. The effectiveness of the transformations is demonstrated with simulations of the cylinder test for PBX 9502 starting with a products EOS for which the CJ detonation speed is 1 per cent too low.

1 Introduction

The wave locus for planar detonation waves in a high explosive (HE) depends on the initial state of the reactants (V_0, e_0) and the products equation of state (EOS). Of most interest is the underdriven or CJ detonation state. In contrast to a shock wave, the state behind a curved detonation wave is not determined by algebraic jump conditions. Rather the detonation state depends on the reaction-zone width and the front curvature. This is known as the curvature effect.

Frequently, simulations do not use a sufficiently fine cell size to resolve the reaction zone. This leads to a numerical curvature effect larger than that corresponding to the HE rate model used for the simulation. It also results in the simulated wave speed of a curved detonation wave being lower than it should [Menikoff, 2014]. In addition, there can be variations in burn rate with HE lots or small inaccuracies in calibrating the products EOS which affect simulated detonation wave speeds.

Due to the curvature effect, the planar CJ detonation wave speed is difficult to measure directly. It can be determined by measuring the diameter effect — detonation wave speed as a function of rate stick diameter — and extrapolating the detonation wave speed to the infinite diameter [Campbell and Engelke, 1976]. For X-0290 (the TATB based development explosive that became PBX 9502), extrapolation of the detonation speed for diameters 12.5 and 25.5 mm linearly in 1/radius gave a CJ detonation speed of 7.70 km/s. Later diameter effect experiments for PBX 9502 by Campbell [1984] included larger diameter rate sticks. Extrapolating the two largest diameters, 50 and 108 mm, gave a CJ detonation speed of $D_{cj} = 7.784$ km/s or 1 % higher than the previous value. The difference results from a rapid change in slope of $D(1/R)$ at large radii caused by a varying reaction-zone width to the sonic point due to carbon clustering in the TATB products. In effect, the sonic point moves from the end of the slow carbon clustering reaction at large radii to near the end of the fast hot spot reaction for moderate to small radii [Menikoff and Shaw, 2012]. Consequently, larger than usual diameter rate sticks are needed to see the asymptotic behavior for the infinite diameter limit.

Here we consider Shaw's products EOS for PBX 9502, see [Menikoff and Shaw, 2012, App. B.2] and references therein. This EOS fits cylinder test data of Pemberton et al. [2011] for the CJ release isentrope very well. However, it was calibrated to the CJ detonation speed from [Campbell and Engelke, 1976], which as noted above is 1 % low. The Shaw EOS is used to illustrate two simple EOS transformations that can be used to fine tune or compensate for errors in the detonation state due to either mesh resolution or small inaccuracies in the products EOS.

The first transformation is a shift in the energy origin, and the second is a linear scaling in the specific volume. By combining the two transformations, the detonation speed can be adjusted

without introducing large errors in the detonation state release isentrope. This is discussed in sec. 2.

To demonstrate the EOS transformations have the desired effect, results of simulations for the cylinder test are discussed in sec. 3. Comparisons between simulated and experimental data for the axial detonation speed and wall velocity show that the CJ detonation speed can be increased by 1 % with only a small effect on the detonation release isentrope.

The main result, summarized in sec. 4, is that the two transformations do allow fine tuning of the products EOS to adjust the CJ detonation speed with minimal side effects on the CJ release isentrope. This can improve the accuracy of the detonation wave speed in simulations.

2 Adjusted products EOS

The heat released by an HE is typically accounted for by the relative offset of the energy origins between the reactants EOS and the products EOS. By convention, the ambient reactants state is usually taken to have $e_0 = 0$. The detonation speed can be adjusted with an additional energy release Q added as a source term in the energy equation

$$\frac{\mathsf{d}e}{\mathsf{d}t} = -P\frac{\mathsf{d}V}{\mathsf{d}t} + Q\frac{\mathsf{d}\lambda}{\mathsf{d}t} \ , \tag{1}$$

where $\frac{\mathsf{d}\lambda}{\mathsf{d}t}$ is the reaction rate. Alternatively, the products EOS can be transformed by shifting the energy origin

$$\tilde{P}(V,e) = P(V,e+Q) \ , \tag{2a}$$
$$\tilde{T}(V,e) = T(V,e+Q) \ . \tag{2b}$$

With Q positive, the detonation locus in the (V,P)–plane is shifted up. This increases the CJ detonation speed. However, a side effect of the increased energy release is to shift the CJ release isentrope up. This increases the speed to which the HE can push a metal plate; *e.g.*, the late time wall velocity in the cylinder test. For fine tuning the detonation speed, Q should be small compared to the heat of detonation, which for an HE is typically 4 to 5 MJ/kg.

The change in the CJ detonation speed D with Q can be estimated from the relation, see [Fickett and Davis, 1979, §3B1], [Wood and Fickett, 1963] and references therein,

$$\frac{\Delta D}{D} = \frac{(\gamma+1)^2}{2\gamma/\Gamma - 1} \cdot \frac{Q}{D^2} \ , \tag{3}$$

where $\gamma = c^2/(P\,V)$ is the adiabatic index and $\Gamma = V(\partial_e P)_V$ is the Grüneisen coefficient, both evaluated at the CJ state (V_{cj}, e_{cj}). For Shaw's 9502 EOS, $\gamma_{cj} = 3.0$ and $\Gamma_{cj} = 0.5$. Then from Eq. (3), $Q = 0.4\,\mathrm{MJ/kg}$ gives a 1 per cent change in D_{cj}. This Q corresponds to about 10 % of the heat of detonation, and as we shall see has a significant effect (6 %) on the cylinder test wall velocity.

Scaling the specific volume V is another transformation that can be used

$$V_f(V) = V_c + f \cdot (V - V_c) \ , \tag{4a}$$

$$\tilde{P}(V, e) = f \cdot P\big(V_f(V), e\big) \ , \tag{4b}$$

$$\tilde{T}(V, e) = T\big(V_f(V), e\big) \ , \tag{4c}$$

$$\tilde{S}(V, e) = S\big(V_f(V), e\big) \ , \tag{4d}$$

where $f > 0$ and $V_c \geq 0$ are parameters. The scaled EOS is thermodynamically consistent. This can be seen by utilizing $\tilde{S}(V, e)$ to define the EOS and using the thermodynamic identity

$$\mathsf{d}S = \frac{1}{T}\,\mathsf{d}e + \frac{P}{T}\,\mathsf{d}V \tag{5}$$

to determine the thermodynamic variables P and T. For fine tuning the CJ detonation speed, $|f - 1|$ should be small; less than 1 or 2 per cent. With $V_c > 0$, the greatest effect of the scale transformation is at very high densities since $P \to \infty$ as $V \to 0$ and $V = 0$ does not correspond to $V_f = 0$. That is not, however, the regime of interest for an HE.

It follows that the Grüneisen coefficient and the sound speed transform as

$$\tilde{\Gamma}(V, e) = \quad V(\partial_e P)_V \quad = \big[f\,V/V_f(V)\big]\,\Gamma\big(V_f(V), e\big) \ , \tag{6a}$$

$$\tilde{c}^2(V, e) = -V^2(\partial_V P)_S = \big[f\,V/V_f(V)\big]^2 c^2\big(V_f(V), e\big) \ . \tag{6b}$$

These are the quantities needed for an iterative algorithm to determine D_{cj} for a given set of parameters f, V_c and Q. We note, if the scaling parameter $V_c = 0$ then the factor $f\,V/V_f(V) = 1$. With $V_c = 0$, the scale transform of an ideal gas EOS is invariant for any f.

From the equation for the Rayleigh line and the sonic condition

$$(\rho_0 D_{cj})^2 = (\rho c_{cj})^2 = (P_{cj} - P_0)/(V_0 - V_{cj}) \ , \tag{7}$$

it can be shown that

$$V_{cj} = \frac{\gamma_{cj}}{\gamma_{cj} + 1 - P_0/P_{cj}}\,V_0 \ , \tag{8a}$$

$$P_{cj} = \frac{\rho_0 D_{cj}^2}{\gamma_{cj} + 1 - P_0/P_{cj}} \ . \tag{8b}$$

Moreover,

$$P_{cj}/V_{cj} = (\rho_0 D_{cj})^2/\gamma_{cj} \ . \tag{8c}$$

We note that substituting Eq. (4) into Eq. (6b) yields

$$\tilde{\gamma}(V,e) = \big[f\,V/V_f(V))\big] \cdot \gamma\big(V_f(V), e\big) \ . \tag{9}$$

Typically, $P_0 \ll P_{cj}$ and can be neglected. Then by Eq. (8a), V_{cj} is determined by γ_{cj}. Unless $\tilde{\gamma}(V_{cj}, e_{cj}) = \gamma(V_{cj}, e_{cj})$, the scale transformation will change the CJ state. The same CJ state would imply $V_f(V_{cj}) = V_{cj}$. Therefore, a scale transformation with $f \neq 1$ will change the CJ state, except for an ideal gas EOS when $V_c = 0$. It is however possible by combining the energy shift and specific volume scaling to obtain the same CJ detonation speed but with the CJ state shifted along the Rayleigh line in the (V,P)–plane; $P = P_0 + (\rho_0 D_{cj})^2(V_0 - V)$.

A closely related alternative to the scale transformation is an isotopic transformation. This can be expressed as a scaling of the Gibbs free energy

$$\tilde{G}(P,T) = f \cdot G(P,T) \ , \tag{10}$$

where f is the ratio of the atomic weight of the isotopes. It has the effect of multiplying specific thermodynamic variables by a constant f. In particular,

$$\tilde{V}(P,T) = f \cdot V(P,T) \ , \tag{11a}$$
$$\tilde{e}(P,T) = f \cdot e(P,T) \ , \tag{11b}$$
$$\tilde{S}(P,T) = f \cdot S(P,T) \ . \tag{11c}$$

For example, $f = 0.5$ could be used with a hydrogen EOS to obtain a deuterium EOS.

For the purpose of adjusting the CJ state, the isotopic transformation can be expressed with independent variables V and e as

$$\tilde{P}(V,e) = P(f \cdot V, f \cdot e) \ , \tag{12a}$$
$$\tilde{T}(V,e) = T(f \cdot V, f \cdot e) \ , \tag{12b}$$
$$\tilde{S}(V,e) = \frac{1}{f} \cdot S(f \cdot V, f \cdot e) \ . \tag{12c}$$

The transformed Grüneisen coefficient and sound speed are

$$\tilde{\Gamma}(V,e) = \tilde{\Gamma}(f \cdot V, f \cdot e) \ , \tag{13a}$$
$$\tilde{c}^2(V,e) = \frac{1}{f} \cdot c^2(f \cdot V, f \cdot e) \ . \tag{13b}$$

We illustrate the behavior of the energy shift and scale or isotopic transformations using Shaw's PBX 9502 EOS with three sets of parameters that increase the CJ detonation speed by about 1 per cent. The CJ states are listed in table 1. The CJ isentrope for the original EOS and the difference with the transformed EOS are shown in fig. 1.

A measure of the HE energy available to do useful work (such as the achievable late time wall velocity for the cylinder test) is the enthalpy change from the initial state to the state on the CJ isentrope with pressure $P_1 = 0.1\,\mathrm{GPa}$, see [Menikoff, 2015, Fig. 1 and Eq. 24]

$$\begin{aligned}
\Delta H &= \int_{P_1}^{P_{cj}} \mathsf{d}P\, V(P, S_{cj}) - \tfrac{1}{2}(P_{cj} - P_0)(V_0 + V_{cj}) \\
&= \int_{V_{cj}}^{V_1} \mathsf{d}V\, [P(V, S_{cj}) - P_1] + (P_{cj} - P_1)\, V_{cj} - \tfrac{1}{2}(P_{cj} - P_0)(V_0 + V_{cj}) \\
&= \int_{V_{cj}}^{V_1} \mathsf{d}V\, P(V, S_{cj}) - \tfrac{1}{2}(P_{cj} - P_0)(V_0 - V_{cj}) + P_0\, V_{cj} - P_1\, V_1 \ . \qquad (14)
\end{aligned}$$

We note that the heat of detonation, the enthalpy change between the initial state and the products at the same pressure and temperature, corresponds to $-\Delta H$ with $P_1 = P_0$ and the

Table 1: CJ detonation state for Shaw's PBX 9502 EOS and for the three transformed EOS. The last columns are the enthalpy change between the initial reactant state and the point on the products CJ isentrope at a pressure $P_1 = 0.1\,\mathrm{GPa}$, Eq. (14), and V at P_1.

Init state	0.52798	0.0	0.0001	0.0		0.0	
D km/s	V cm^3/g	e MJ/kg	P GPa	u_p km/s		ΔH MJ/kg	$V_{cj}(P_1)$ cm^3/g
	original EOS						
7.700	0.39611	1.847	28.02	1.922		2.794	3.4207
	transform 1: scaled, $V_c = 0.52798$, $f = 1.01333$				$Q = -0.09$		
7.782	0.39807	1.743	28.22	1.915		2.742	3.3219
	transform 2: isotopic, $f = 0.99$				$Q = -0.075$		
7.786	0.39630	1.810	28.63	1.942		2.772	3.3154
	transform 3:				$Q = 0.5$		
7.790	0.39488	2.428	28.98	1.964		3.115	3.8710

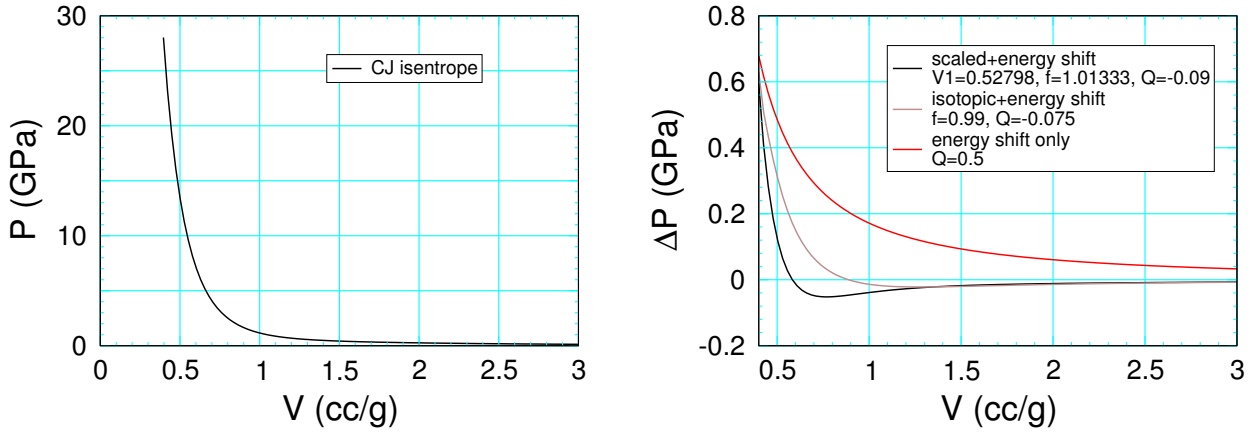

Figure 1: Comparison of CJ isentropes for transformed products EOS. Left plot is CJ release isentrope for Shaw's PBX 9502 EOS. Right plot is the pressure difference between CJ isentropes for the three transformed EOS and the original EOS.

addition of the thermal energy $-C_p \cdot (T_1 - T_0)$, where C_p is the specific heat at constant pressure. It can be larger than the work an application can extract from the HE by as much as 30 %.

For a given change in the detonation speed, the table shows that the enthalpy change is significantly larger for the pure energy shift then for the scaled or isotopic transformations with an energy shift. This is largely due to the larger area under the pressure difference curve. In addition to ΔP being smaller for the two transformations compared to the energy shift only, there is a change in the sign of ΔP that further reduces the integral in Eq. (14). We note, however, that even for the same ΔH, the area under the pressure difference curve is not necessarily 0. This is because the right hand side of Eq. (14) also depends on the CJ state and the state at the low pressure cutoff, both of which vary with the transformations.

3 Cylinder test simulations

Data from the cylinder test is used in calibrating the products EOS. In particular, the wall velocity is related to the release isentrope behind the detonation wave. It is a good application to illustrate the effect of the transformations on the products EOS.

Simulations of the cylinder test have been performed using the `xRage` code with the SURFplus reactive burn model for PBX 9502 and the products EOS discussed in the previous section. PBX 9502 has fast and slow burn rates associated with hot-spot reaction and carbon clustering, respectively. Utilizing an adaptive mesh to 0.025 mm the fast rate part of the reaction zone

contained about 6 cells. The slow rate portion of the reaction zone (slightly under 3 mm) is well resolved. Simulated results will be compared with experimental data

Pemberton et al. [2011] did a series of 9 1-inch diameter cylinder test experiments. The PBX 9502 used in the experiments came from 3 lots and had a density variation of 0.3 %. The shots were fired outdoors with temperature variation from 70 to 78 F. The average axial detonation speed of 7.620 had a shot-to-shot variation of ±0.046 km/s, which is over 10 times larger than for the diameter effect experiments of Campbell [1984]. The detonation speed variation is mostly due to the different 9502 lots. For each lot of 9502, there were 3 experiments which had a smaller temperature variation, only 3 F, and a detonation speed variation of ±0.006 km/s; about 0.1 %.

Each experiment had 8 PDV probes at different axial locations and 3 azimuthal angles. Figure 2 shows a comparison of the wall velocity for each 9502 lot from 3 probes located at

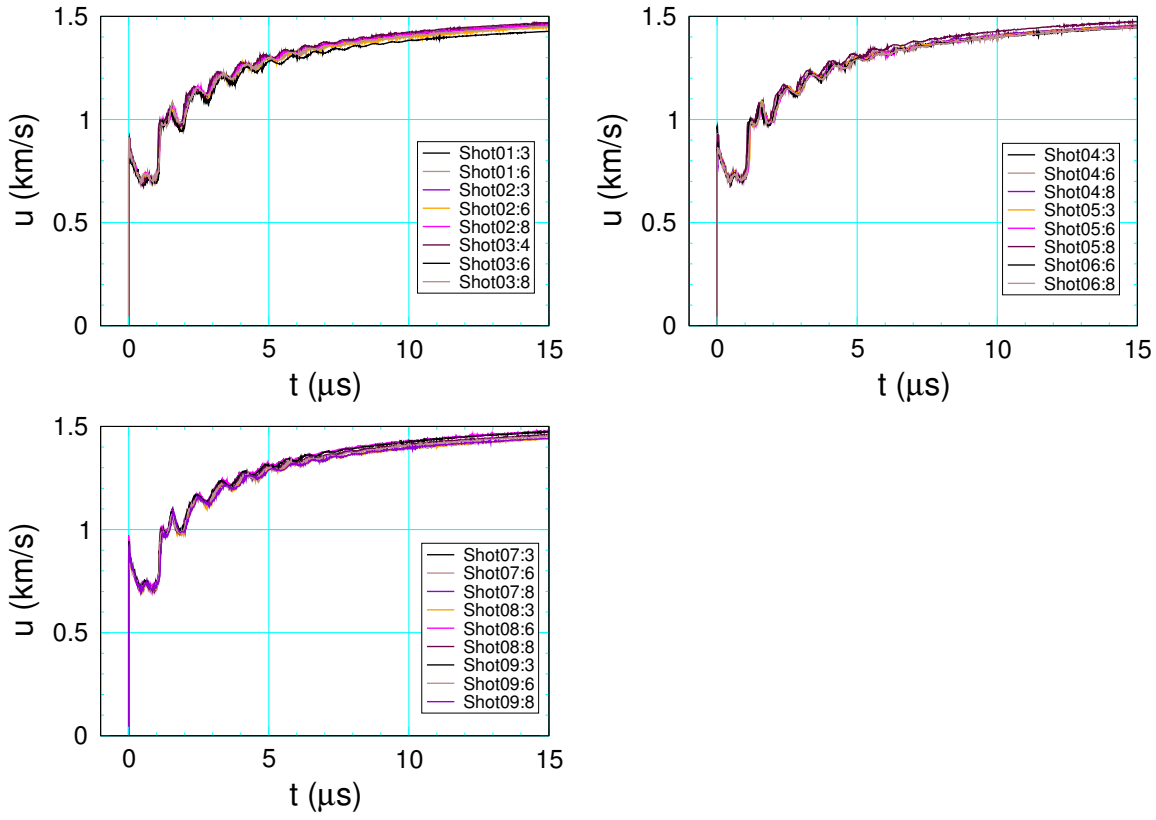

Figure 2: Comparison of cylinder test wall velocity for 3 lots of PBX 9502 from experiments by Pemberton et al. [2011]. For each lot there were 3 experiments. Shown here are 3 probes for each shot approximately at the middle of the 10 inch long tube and separated azimuthally by 120 degrees.

approximately the middle of the 10 inch long cylinder and separated azimuthally by 120 degrees. At late times, corresponding to a factor of 3 expansion of the wall radius, the wall velocity varies by about $\pm 1\,\%$. This maybe due to the strength properties of the copper wall (such as spall) rather than the properties of the 9502 per se. The variations in the data for the detonation speed and wall velocity give rise to inaccuracies in calibrating a products EOS, hence, the need to fine tune the EOS. We also note that at a factor of 3 expansion, the pressure of the products is a few tenths of GPa. Hence, the cutoff of the enthalpy difference in Eq. (14).

Simulation of the cylinder test were performed with each of the transformed products EOS listed in table 1. Figure 3 shows that the 3 transformed EOS with increased CJ detonation speed also has the desired effect of increasing the axial detonation speed. Figure 4 shows the effect of the EOS on the simulated wall velocity. The scaled and isotopic transformed EOSs, with nearly the same ΔH as the original EOS, have a small effect on the wall velocity. In contrast, the energy shift only transformation that increases ΔH also increases the wall velocity.

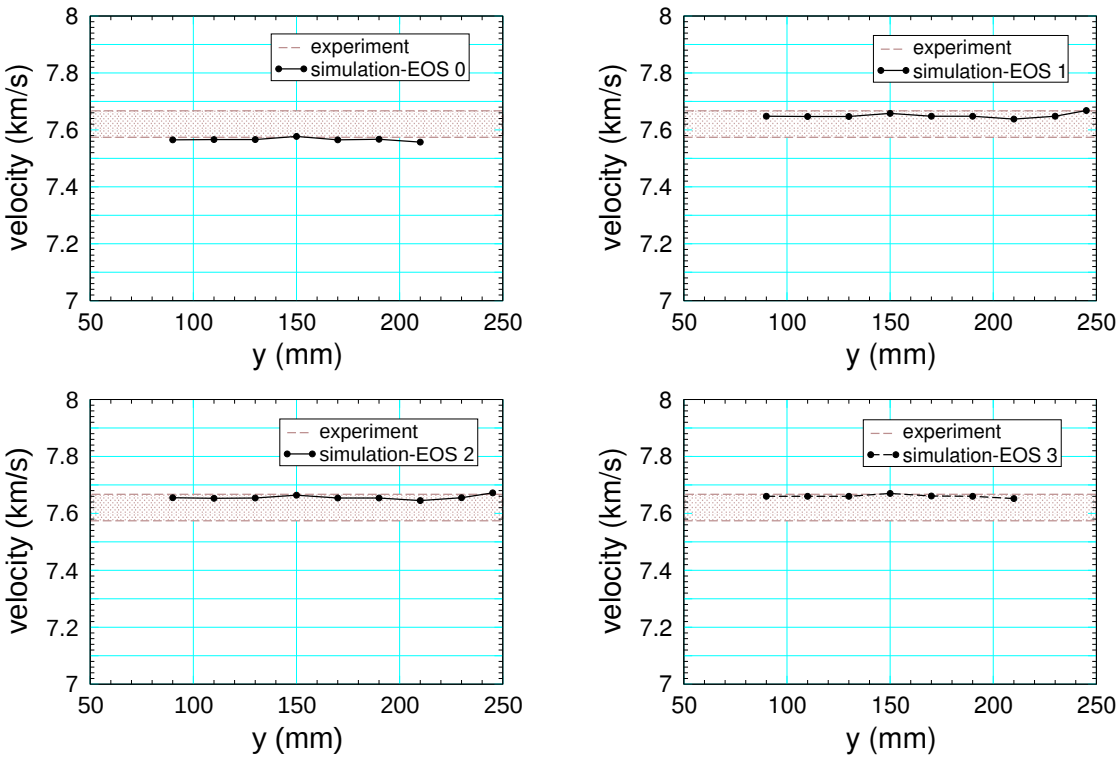

Figure 3: Axial detonation speed for simulations of cylinder test with product EOS listed in table 1. The brown shaded band corresponds to the range for shot-to-shot variations of cylinder test experiments.

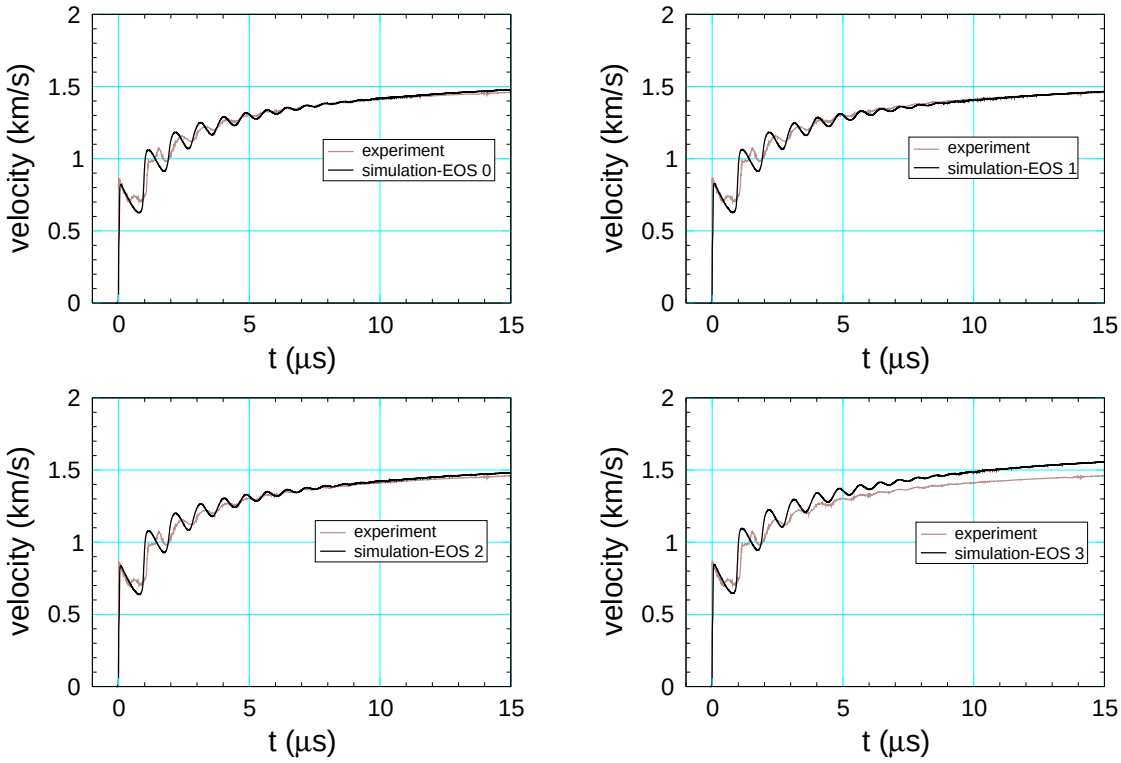

Figure 4: Wall velocity for experimental and simulated cylinder test experiments. Simulations used product EOS listed in table 1.

We note two complication with the axial velocity for the cylinder test. First, the low end of Pemberton's experimental detonation speed variation, 7.574 km/s, is slightly below the detonation speed Campbell [1984] measured for an unconfined 1-inch diameter rate stick. The copper confinement of the HE in the cylinder test is expected to increase the axial detonation speed. The discrepancy is largely due to the different 9502 lots used in the experiments; see [Hill and Aslam, 2010, fig. 6] for the variation of the curvature effect with lot. The detonation speed variation may also in part be due to a small air gap ($\sim$ 1 mil) between the 9502 and the copper wall. The gap is 10 to 15 % of the fast rate part of the reaction-zone width, and may affect the confinement, and hence the detonation front curvature and the detonation speed.

Second, the model burn rate determines the reaction-zone width, which affects the magnitude of the curvature effect and hence the numerical detonation speed; see [Menikoff, 2014]. Similarly, the burn rate may vary among HE lots (since the hot spot distribution can vary with the grain scale heterogeneities in a PBX), and hence the experimental curvature effect and the cylinder test axial detonation speed.

4 Summary

The detonation speed depends on the products EOS and the curvature effect. Physically the magnitude of the curvature effect depends on the reaction-zone width. Both the model EOS and the mesh resolution affect the detonation speed of a simulation. Uncertainties in data and the EOS calibration can lead to inaccuracies in the detonation state. The reaction zone is typically small and under-resolved. This can lead to a numerical reaction-zone width larger than the physical reaction-zone width. Hence, a numerical curvature effect larger than the physical curvature effect [Menikoff, 2014] and inaccuracies in the detonation speed.

Using the cylinder test as an illustrative example, we have shown that the products EOS can be fine tuned to adjust or compensate for inaccuracies in the CJ detonation speed with minimal effect on HE energy available to do useful work. The EOS is fine tuned with two transformation:

i. Shifting the energy orgin.

ii. Linear scaling of the specific volume or an isentropic scaling.

The combined transformation is thermodynamically consistent.

The `xRage` code has input parameters for an extra energy release Q (equivalent to shifting the products energy origin) and the isotopic scale transformation parameter $f_x = 1/f$. These two parameters can be used to adjust both the detonation speed and the change in enthalpy (from the initial state to a point on the CJ release isentrope at a suitable low pressure); see contours in fig. 5. The contours of both D and h are nearly straight lines since the changes to both D_{cj} and h are small (less than 2 %) and linearization is a good approximation. For the cylinder test, this can be used for small corrections to both the detonation speed and the wall velocity.

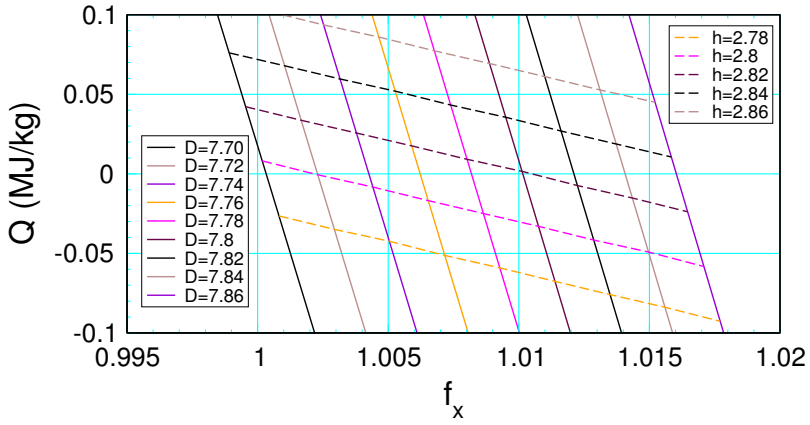

Figure 5: Contours for D and h in the (f_x,Q)-plane for PBX 9502. The slope for constant D is $\Delta Q/\Delta f_x \approx -54$ and for constant h is $\Delta Q/\Delta f_x \approx -3.8$.

References

A. W. Campbell. Diameter effect and failure diameter of a TATB based explosive. *Propellants, Explosives, Pyrotechnics*, 9:183–187, 1984. 2, 8, 10

A. W. Campbell and R. Engelke. The diameter effect in high-density heterogeneous explosives. In *Proceeding of the Sixth International Symposium on Detonation*, pages 642–652, 1976. 2

W. Fickett and W. C. Davis. *Detonation*. Univ. of Calif. Press, 1979. 3

L. G. Hill and T. D. Aslam. Detonation shock dynamics calibration for PBX 9502 with temperature, density and material lot variation. In *Proceeding of the Fourteenth International Symposium on Detonation*, pages 779–788, 2010. 10

R. Menikoff. Effect of resolution on propagating detonation wave. Technical Report LA-UR-14-25140, Los Alamos National Laboratory, 2014. URL http://dx.doi.org/10.2172/1136940. 2, 10, 11

R. Menikoff. JWL equation of state. Technical Report LA-UR-15-29536, Los Alamos National Lab., 2015. URL https://www.osti.gov/scitech/servlets/purl/1229709. 6

R. Menikoff and M. S. Shaw. The SURF model and the curvature effect for PBX 9502. *Combustion Theory And Modelling*, pages 1140–1169, 2012. URL http://dx.doi.org/10.1080/13647830.2012.713994. 2

S. Pemberton, T. Sandoval, T. Herrera, and J. Echave. Test report for equation of state measurements of PBX 9502. Technical Report LA-UR-11-04998, Los Alamos National Lab., 2011. 2, 8

W. W. Wood and W. Fickett. Investigation of the Chapman-Jouguet hypothesis by the "Inverse Method". *Phys. Fluids*, 6, 1963. URL http://dx.doi.org/10.1063/1.1706795. 3